FLUID FILM BEHAVIOUR IN A CYLINDRICAL BORE JOURNAL BEARING

Dewan Mohammad Nuruzzaman *
Department of Mechanical Engineering
Bangladesh Institute of Technology (BIT), Dhaka, Gazipur –1700

Abstract A theoretical analysis of a high speed cylindrical bore journal bearing behaviour is presented in this paper. In calculating the design parameters of the bearing such as load capacity, side leakage and power loss, finite element method is used. In completing the solution procedure, an isoviscous, incompressible, Newtonian fluid is considered and isothermal analysis has been carried out. The effects of variations in operating variables such as eccentricity ratio and shaft speed on the bearing design parameters have been calculated. In order to check the validity, these results are compared with the available published results. The comparison shows a satisfactory agreement which confirms the basis of the numerical model.

Keywords: *Wear, Hydrodynamic Lubrication,Journal Bearing, Finite Element Method*.

INTRODUCTION

Lubrication problems appear often in engineering design and it is the mechanism that separates two surfaces moving relative to each other by a fluid film which can be sheared with low resistance without causing any damage to the surfaces. Wear is the major cause of material wastage and loss of mechanical performance of machine elements, and any reduction in wear can result in considerable savings which can be made by improved friction control. Lubrication is an effective means of controlling wear and reducing friction, and it has wide applications in the operation of machine elements such as bearings. When the surfaces in relative motion are so oriented that the motion causes the fluid pressure to support the load without metal-to-metal contact, the lubrication phenomenon is known as hydrodynamic lubrication. A common engineering component which exploits this principle is the cylindrical bore journal bearing in which a loaded shaft (or journal) rotates in a metallic bush that is fed continuously by a lubricating fluid. The principles of hydrodynamic lubrication were first established by a well known scientist Osborne Reynolds in 1886. He explained the mechanism of hydrodynamic lubrication through the generation of a viscous liquid film between the moving surfaces. The entire process of hydrodynamic pressure generation can be described mathematically to enable accurate prediction of bearing characteristics and numerical analysis has allowed models of hydrodynamic lubrication to describe the characteristics of real bearings.

*Email: dewan98@hotmail.com

BACKGROUND

Lubrication is the mechanism that reduces friction between two surfaces in relative motion. Power loss, excessive temperature rise and consequent wear are the problems associated with friction. The serious appreciation of hydrodynamic lubrication started towards the end of the 19th century. Among all the early investigations in lubrication, Beauchamp Tower's experiments represented a breakthrough that led to the development of lubrication theory. The analysis of this work carried out by Stokes and later Reynolds led to a theoretical explanation of Tower's results and on this the theory of fluid film lubrication has been based. In 1886, with the publication of classical paper on hydrodynamic lubrication, Reynolds proved that hydrodynamic pressure of liquid entrained between sliding surfaces was sufficient to prevent contact between surfaces even at very low sliding speed. The work of Reynolds initiated many other research efforts aimed at improving the interaction between two contacting surfaces, and which continue up till today. As a result, journal bearings are now designed to high levels of sophistication. After World War II, a general trend in mechanical engineering towards higher loads, higher velocities and higher operating temperatures was observed in connection with attempts to reduce the weights of the moving parts in machinery.

Numerical analysis has allowed models of hydrodynamic lubrication to include closer approximations to the characteristics of real bearings. Numerical solutions to hydrodynamic lubrication problems can now satisfy most engineering requirements for prediction of bearing characteristics.

To analyze bearing design parameters, several approximate numerical methods have evolved over the years such as the finite difference method and the finite element method. The finite difference method is difficult to use when irregular geometries are to be solved. Nowadays finite element method becomes more popular for numerical modeling. Complex geometrical configurations and abrupt changes in field properties are often encountered in fluid film lubrication. In these cases, the finite difference method is inherently difficult to apply because irregular meshes should be employed. Conversely, the finite element method can overcome these difficulties. Use of elements and interpolation functions ensure continuity of pressure and mass flow rate across inter-element boundaries. The finite element method has been used in the solution of fluid film lubrication problems for some years. Booker and Huebner (1972) used finite element method for the solution of hydrodynamic lubrication problems. Later Hayashi and Taylor (1980) used the finite element technique to predict the characteristics of a finite width journal bearing. A theoretical investigation was carried out by Gethin and Medwell (1984) using the finite element method for a high speed bearing. A theoretical study based on the finite element method was carried out to investigate the performance of a twin-axial groove cylindrical bore bearing (Gethin and Deihi,1987). Basri and Gethin (1990) worked on the finite element method for the solution of hydrodynamic lubrication problems. A theoretical and experimental study of thermal effects in a plain circular steadily loaded journal bearing was carried out by Ma and Taylor (1992). More recently, Gethin (1996) worked on the thermal behaviour of various types of high speed journal bearings.

The purpose of this paper is to present comprehensive performance characteristics of a high speed journal bearing for a range of eccentricity ratio and shaft speed. The results are shown in graphical style. The carpet plots of load capacity, side leakage and power loss may be utilized directly in other design procedures.

THEORETICAL ANALYSIS AND NUMERICAL COMPUTATION

The finite element method (FEM) has been used for the numerical modeling of a cylindrical bore journal bearing to calculate design parameters such as load capacity, side leakage and power loss. In this analysis, to discretize the governing Reynolds equation, Galerkin weighted residual approach has been adopted. In the numerical model, a finite element mesh was considered. The load bearing film was divided into a finite number of eight-node isoparametric elements of serendipity family . In the numerical solution, appropriate boundary condition was applied. The overall solution procedure was completed by iteration and pressure field had converged, and finally the usual bearing design parameters such as load capacity, side leakage and power loss were calculated.

Formulation of governing equation

The governing Reynolds differential equation is :

$$\frac{\partial}{\partial x}(h^3\frac{\partial p}{\partial x})+\frac{\partial}{\partial y}(h^3\frac{\partial p}{\partial y})=6U\mu\frac{dh}{dx}$$

$$\text{or,}\frac{\partial}{\partial x}(\frac{h^3}{12\mu}\frac{\partial p}{\partial x})+\frac{\partial}{\partial y}(\frac{h^3}{12\mu}\frac{\partial p}{\partial y})=\frac{U}{2}\frac{dh}{dx} \qquad [1]$$

Now by the Galerkin weighted residual method, the residual over the domain is :

$$\tilde{R}=\frac{\partial}{\partial x}(\frac{h^3}{12\mu}\frac{\partial \tilde{p}}{\partial x})+\frac{\partial}{\partial y}(\frac{h^3}{12\mu}\frac{\partial \tilde{p}}{\partial y})-\frac{U}{2}\frac{dh}{dx}\neq 0 \quad [2]$$

where $\tilde{p}$ is the approximate solution very close to the exact solution p.

Now for Reynolds equation :

$$\int_{\Omega}\left[\frac{\partial}{\partial x}\left(\frac{h^3}{12\mu}\frac{\partial p}{\partial x}\right)+\frac{\partial}{\partial y}\left(\frac{h^3}{12\mu}\frac{\partial p}{\partial y}\right)-\frac{U}{2}\frac{dh}{dx}\right]\phi_i d\Omega=0$$

where ϕ_i is the shape function.

Writing these equations in general matrix form :

$$\begin{bmatrix} K_{11}\ K_{12}.....K_{18} \\ K_{21}\ K_{22}.....K_{28} \\ .\ .\ . \\ .\ .\ . \\ K_{81}\ K_{82}.....K_{88} \end{bmatrix}\begin{Bmatrix} a_1 \\ a_2 \\ . \\ . \\ a_8 \end{Bmatrix}=\begin{Bmatrix} F_1 \\ F_2 \\ . \\ . \\ F_8 \end{Bmatrix} \qquad [3]$$

where the expressions for the stiffness and load terms are respectively :

$$K_{ij}=\int_{\Omega}\frac{h^3}{12\mu}\left[\frac{\partial\phi_i}{\partial x}\frac{\partial\phi_j}{\partial x}+\frac{\partial\phi_i}{\partial y}\frac{\partial\phi_j}{\partial y}\right]d\Omega \qquad [4]$$

$$F_i=\int_{\Omega}\phi_i\frac{U}{2}\frac{dh}{dx}d\Omega \qquad [5]$$

Each shape function is a Lagrange quadratic polynomial which satisfies the interpolation property:

$$\phi_j(x_i,y_i)=\delta_{ji} \qquad [6]$$

where the interpolation property (Akin,1984) requires that

$$\begin{aligned}\phi_1(\xi_1,\eta_1) &= 1 \\ \phi_1(\xi_j,\eta_j) &= 0 \qquad j\neq 1\end{aligned} \qquad [7]$$

The Jacobian matrix is given by :

$$J(\xi,\eta)=\begin{bmatrix} \frac{\partial x}{\partial \xi} & \frac{\partial y}{\partial \xi} \\ \frac{\partial x}{\partial \eta} & \frac{\partial y}{\partial \eta} \end{bmatrix}=\begin{bmatrix} J_{11}(\xi,\eta) & J_{12}(\xi,\eta) \\ J_{21}(\xi,\eta) & J_{22}(\xi,\eta) \end{bmatrix}$$

The determinant of the Jacobian matrix $\left| J(\xi,\eta) \right|$ is called the Jacobian. Hence :

$$\left| J(\xi,\eta) \right| = \frac{\partial x}{\partial \xi}\frac{\partial y}{\partial \eta} - \frac{\partial x}{\partial \eta}\frac{\partial y}{\partial \xi} \qquad [8]$$

so that , $\left| J(\xi,\eta) \right| > 0$

From the definition of Jacobian matrix :

$$\left[J(\xi,\eta)\right]^{-1}=\frac{1}{\left|J(\xi,\eta)\right|}\begin{bmatrix} \frac{\partial y}{\partial \eta} & -\frac{\partial y}{\partial \xi} \\ -\frac{\partial x}{\partial \eta} & \frac{\partial x}{\partial \xi} \end{bmatrix} \qquad [9]$$

So the stiffness and load integral terms are :

$$K_{ij} = \int_{-1}^{1}\int_{-1}^{1} \frac{h^3}{12\mu}\frac{\partial \phi_i}{\partial x}\frac{\partial \phi_j}{\partial x}\left|J(\xi,\eta)\right| d\xi\, d\eta$$

$$+ \int_{-1}^{1}\int_{-1}^{1} \frac{h^3}{12\mu}\frac{\partial \phi_i}{\partial y}\frac{\partial \phi_j}{\partial y}\left|J(\xi,\eta)\right| d\xi\, d\eta \qquad [10]$$

$$F_i = \int_{-1}^{1}\int_{-1}^{1} \frac{U}{2}\frac{dh}{dx}\left|J(\xi,\eta)\right| d\xi\, d\eta \qquad [11]$$

Using equations [10] and [11], equation [3] is solved for bearing design parameters such as load capacity, side leakage and power loss.

RESULTS AND DISCUSSION

In calculating the performance characteristics presented here for a high speed cylindrical bore journal bearing, an isoviscous, incompressible, Newtonian fluid was considered. The hydrodynamic solution uses a viscosity equal to that of an oil of ISO viscosity grade 32.

Figure 1 illustrates the dimensionless load variation at different eccentricity ratio for R=50 mm, C/R=0.004, L/R=1.0 and Re=1000. From the finite element results it was apparent that at low eccentricity ratio, the dimensionless load increased gradually but it was greatly increased with high eccentricity ratio. The comparison of these results with Gethin and Deihi's results showed very good agreement and about 90% accuracy was achieved. Figure 2 shows the variation of load capacity with shaft speed ranging from 5000 rpm to 20000 rpm for R=50 mm, L/R=1.0, C/R=0.004 and eccentricity ratio = 0.7. From the finite element results it was clear that the load capacity increased gradually with the increase of shaft speed. The comparison of these results with those presented by Gethin and Medwell showed good agreement and about 80 % accuracy was obtained. Figure 3 shows the variation of dimensionless side leakage with eccentricity ratio for R = 50 mm, L/R = 1.0, C/R = 0.004 and Re = 1000. The finite element results revealed that the dimensionless side leakage was not affected significantly by eccentricity ratio and it increased steadily with the increase of eccentricity ratio. In comparison with Gethin and Deihi's results, the finite element results showed good agreement and about 85 % accuracy was achieved. Figure 4 exhibits the variation of the side leakage with the shaft speed ranging from 5000 rpm to 20000 rpm for R = 50 mm, L/R = 1.0, C/R = 0.004 and eccentricity ratio = 0.7. From the finite element results it was quite clear that shaft speed had a profound effect on the side leakage and it increased remarkably with the increase of the shaft speed. In comparison with the results obtained by Gethin and Medwell, the finite element results showed similar trends and about 80 % accuracy was obtained. The variation of dimensionless power loss with eccentricity ratio for R = 50 mm, L/R = 1.0, C/R = 0.004 and Re = 1000 is shown in Figure 5. The finite element results described that at low eccentricity ratio dimensionless power loss was not significantly affected and it increased remarkably with high eccentricity ratio. In comparison with Gethin and Deihi's results, finite element results showed good agreement and about 85 % accuracy was achieved. The variation of power loss with shaft speed ranging from 5000 rpm to 20000 rpm for R = 50 mm, L/R = 1.0, C/R = 0.004 and eccentricity ratio = 0.7 is shown in Figure 6. From the finite element results, it was quite clear that the shaft speed had a significant effect on the power loss variation and it increased greatly with the increase of shaft speed because as the speed became greater the viscous shearing increased rapidly. In comparison with the results presented by Gethin and Medwell, finite element results showed similar trends of variation and about 80 % accuracy was obtained. Figure 7 illustrates the results of computation for R = 50 mm, L/R = 1.0, and C/R = 0.004. Calculations were carried out for power loss and load capacity over a range of eccentricity ratio and shaft speed. From the graphs it is quite clear that power loss is not affected significantly by eccentricity ratio and it increases steadily with the increase of eccentricity ratio. Also it was seen that shaft speed influenced power loss very significantly and it increased remarkably with the increase of shaft speed because as the speed became greater, the viscous shearing increased rapidly. Figure 8 exhibits the variation of side leakage and load capacity for a range of eccentricity ratio and shaft speed. From

the graphs it is apparent that side leakage is not influenced significantly by eccentricity ratio, but shaft speed has a profound effect on side leakage and it increases greatly with the increase of shaft speed. For the load capacity, the graphs show that at low eccentricity ratio and shaft speed, the load capacity is low whereas with the increase of eccentricity ratio and shaft speed, the load capacity increases remarkably. Figure 9 shows the results of computation for the variation of power loss and load capacity with eccentricity ratio and shaft speed for R=50 mm, L/R = 0.5 and C/R = 0.002. From the graphs it is seen that power loss is not affected markedly by eccentricity ratio but shaft speed has a significant effect on the power loss variation and it increases greatly with the increase of shaft speed. Figure 10 illustrates the variation of side leakage and load capacity with eccentricity ratio and shaft speed. From the obtained results it was quite clear that the side leakage was not affected significantly by eccentricity ratio but it increased greatly with the increase of the shaft speed. The results also showed that at low eccentricity ratio and shaft speed, the load capacity was low, but at high eccentricity ratio and shaft speed, load capacity increased greatly. Computational results are also shown in Figure 11 for R=50 mm, L/R = 1.5 and C/R = 0.002. From the graphs it is quite clear that power loss is not affected significantly by eccentricity ratio, but shaft speed has a profound effect on power loss variation because as the shaft speed becomes greater, the viscous shearing increases rapidly. From the graphs, it is also clear that at low eccentricity ratio and shaft speed, load capacity is low but with the increase of eccentricity ratio and shaft speed, the load capacity increases remarkably. Figure 12 illustrates the results of computation for the variation of side leakage and load capacity with eccentricity ratio and shaft speed. From the graphs it is apparent that side leakage is not affected significantly by eccentricity ratio, but it increases remarkably with the increase of shaft speed. Also it is quite clear that at low eccentricity ratio and shaft speed, the load capacity is low, but at high eccentricity ratio and shaft speed, the load capacity increases greatly.

CONCLUSIONS

In order to calculate bearing design parameters, finite element method has been used. The effects of operating variables such as eccentricity ratio and shaft speed on the bearing design parameters such as load capacity, side leakage and power loss were calculated. In order to check the validity when these results were compared with the available published results, the agreement was found quite satisfactory which confirms the hydrodynamic basis of the present numerical model. Furthermore, results are shown by carpet plots which can be used for design purposes.

REFERENCE

Basri, S. and Gethin, D.T., " A Comparative Study of the Thermal Behaviour of Profile Bore Bearings", Tribology International. 4(12): 265-276 (1990).

Booker, J.F., and Huebner, K.H., "Application of Finite Elements to Lubrication": An Engineerimg Approach. Journal of Lubrication Technology, Trans. ASME. 24(4): 313-323 (1972).

Gethin, D.T. "Behaviour of High Speed Journal Bearings". Tribology International 29(7): 579-596 (1996).

Gethin, D.T., and Medwell, J.O., "An Investigation into the Performance of a High Speed Journal Bearing with two Axial Lubricant Feed Grooves". Project Report, University of Wales (1984).

Gethin, D.T. and Deihi, M.K.I., "Effect of Loading Direction on the Performance of a Twin Axial Groove Cylindrical Bore Bearing". Tribology International. 20: 179-185 (1987).

Hayashi, H. and Taylor, C.M., "A Determination of Cavitation Interfaces in Fluid Film Bearings Using Finite Element Analysis". Journal Mechanical Engineering Science. 22(6): 277-285 (1980).

Ma, M.T. and Taylor, C.M., "A Theoretical and Experimental Study of Thermal Effects in a Plain Circular Steadily Loaded Journal Bearing". Transactions IMechE. 824(9): 31-44 (1992).

Wada, S. and Hayaski, H., " Application of the Finite Element Method to Hydrodynamic Lubrication Problems". Bulletin of Japan Society of Mechanical Engineers. 14(77): 1234-1244 (1971).

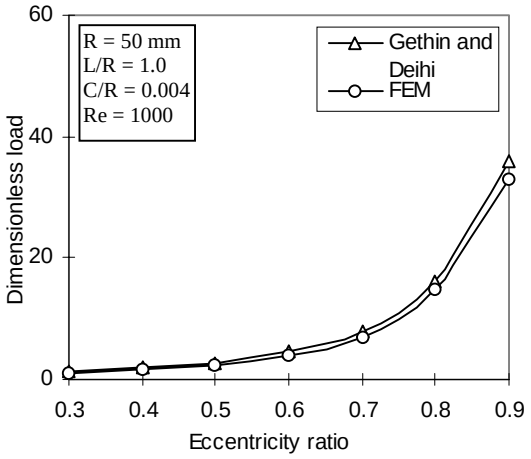

Figure 1: Variation of dimensionless load with eccentricity ratio.

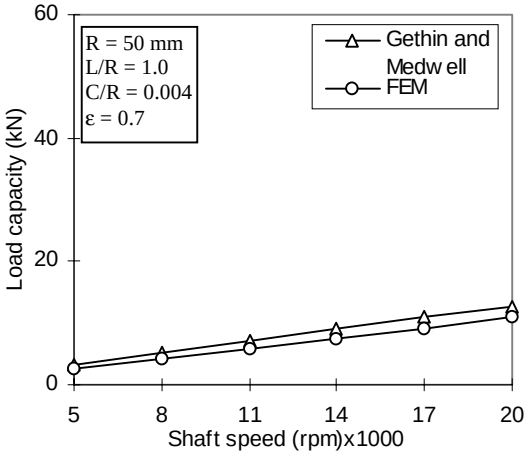

Figure 2: Variation of load capacity with shaft speed

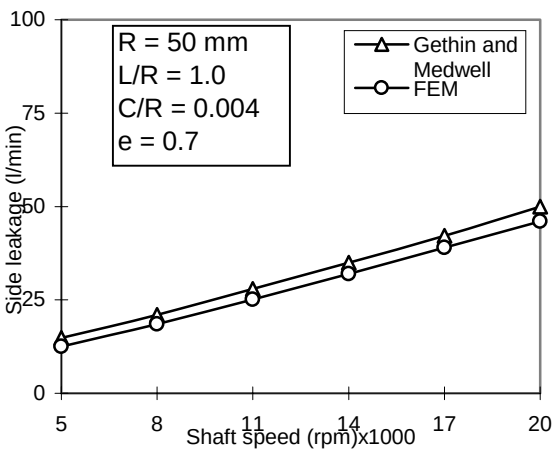

Figure 4: Variation of side leakage with shaft speed.

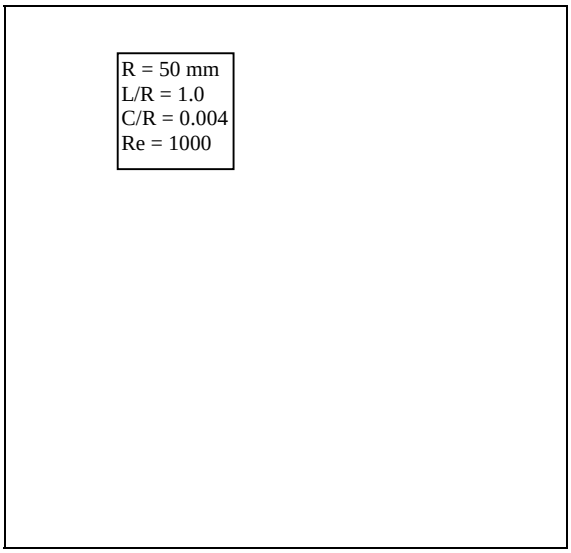

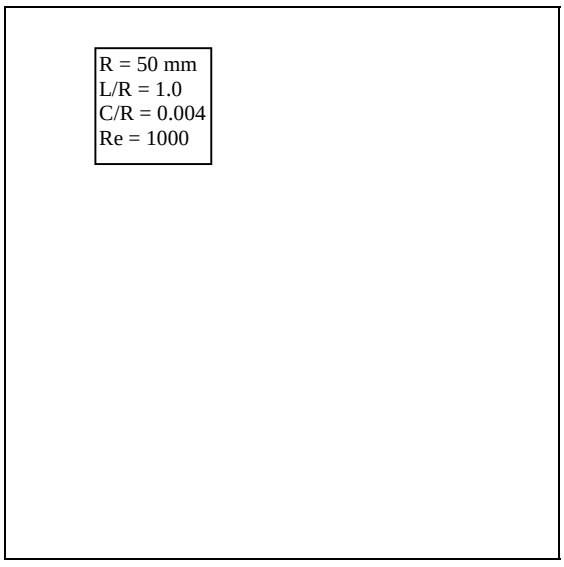

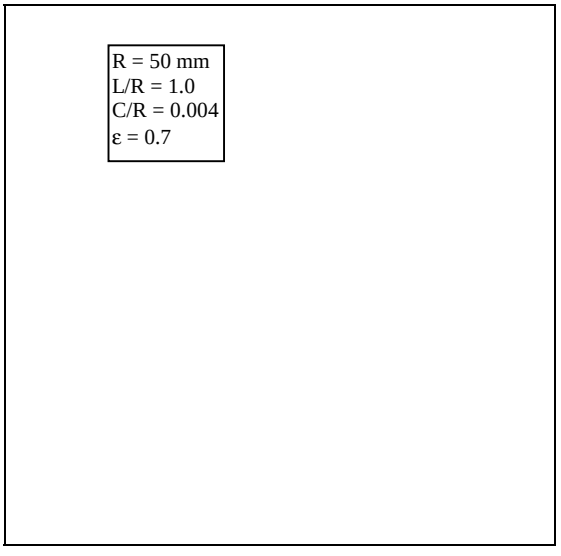

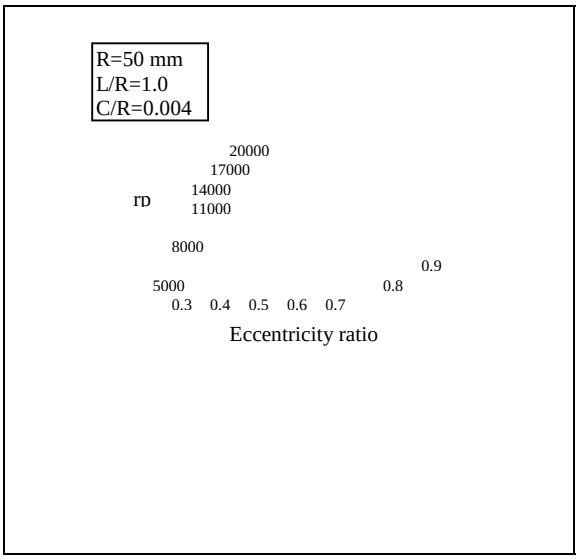
R=50 mm
L/R=1.0
C/R=0.004
rp
20000
17000
14000
11000
8000
5000
0.3
0.4
0.5
0.6
0.7
0.8
0.9
Eccentricity ratio

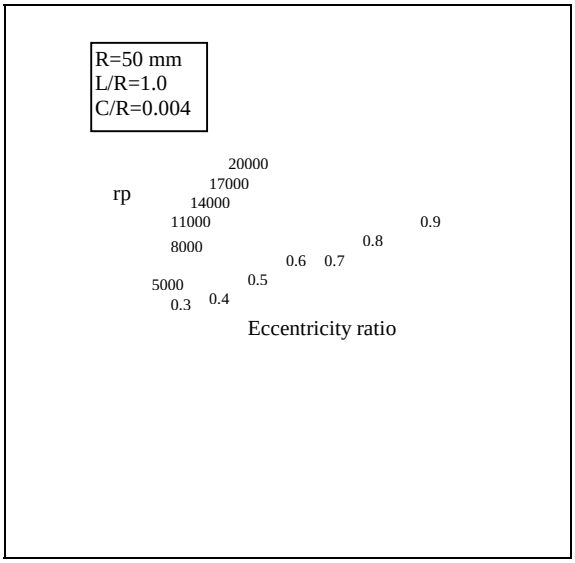
R=50 mm
L/R=1.0
C/R=0.004
rp
20000
17000
14000
11000
8000
5000
0.3
0.4
0.5
0.6
0.7
0.8
0.9
Eccentricity ratio

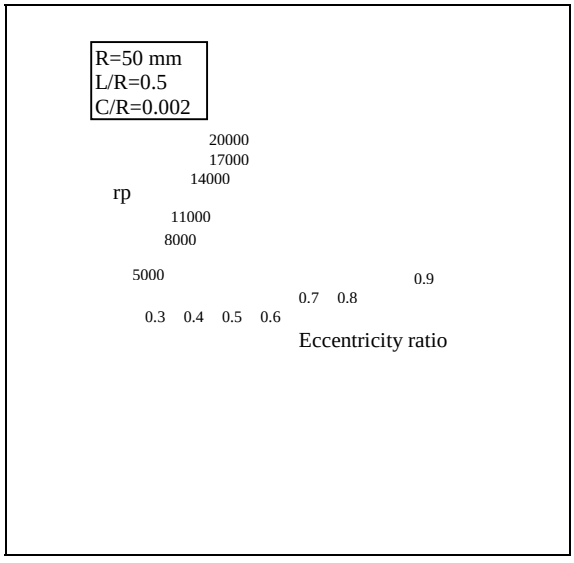
R=50 mm
L/R=0.5
C/R=0.002
rp
20000
17000
14000
11000
8000
5000
0.3
0.4
0.5
0.6
0.7
0.8
0.9
Eccentricity ratio

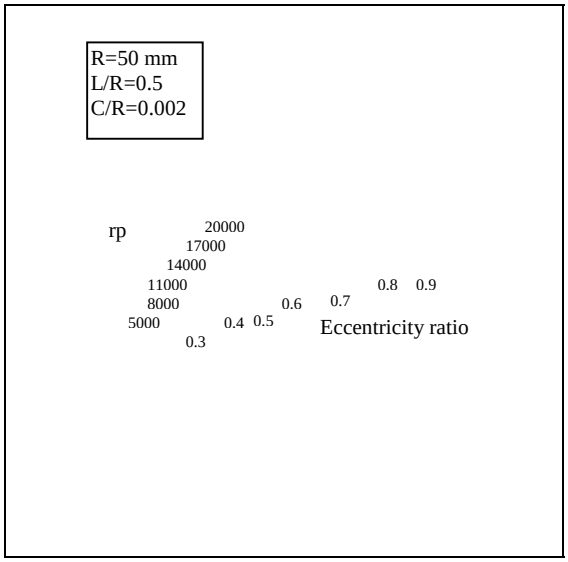

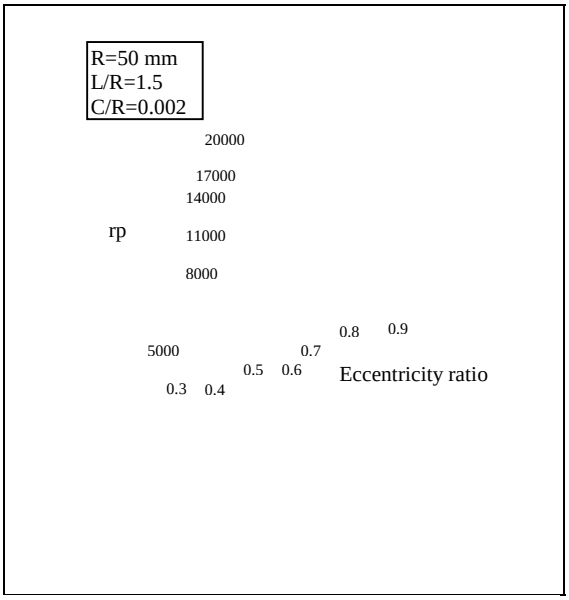

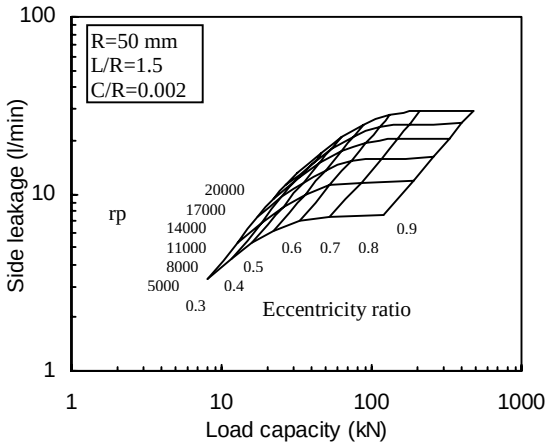

Figure 12: Variation of side leakage and load capacity w ith eccentricity ratio and shaft speed